Rigorous Analysis of Electromagnetic Scattering by Grating of Plasmonic Nanorods Coupled to Magneto-Optical Slab

Vakhtang Jandieri[1], Kiyotoshi Yasumoto[2], *Fellow, IEEE*, and Jaromir Pistora[3]

[1]General and Theoretical Electrical Engineering (ATE), Faculty of Engineering, University of Duisburg-Essen, and CENIDE – Center for Nanointegration Duisburg-Essen, D-47048 Duisburg, Germany
[2]Faculty of Information Science and Electrical Engineering, Kyushu University, Fukuoka 819-0395, Japan
[3]Nanotechnology Centre, VŠB-Technical University of Ostrava, 708 33 Ostrava, Czech Republic

A rigorous self-contained formulation for analyzing electromagnetic scattering by a grating of plasmonic nanorods (Ag) coupled to a magneto-optical slab is presented. Bi-substituted gadolinium iron garnet is considered as the magneto-optical material. We measured the dielectric permittivity of the iron garnet and utilized the experimental data in our analyses. The method uses the Lattice Sums technique combined with the generalized reflection matrix approach. Using the method, the spectral response in reflectance as well as near-field distributions at resonance wavelengths have been numerical studied. Special attention has been paid to the coupling mechanism between the plasmonic grating and the magneto-optical slab. Physical insight is given to the strong field enhancement inside the magneto-optical material due to coupling with the plasmonic grating. Generalization of the method to the multilayered sandwiched structures, where the metal layer supporting surface plasmons is in contact with a layer possessing magnetically induced anisotropy, is straightforward. Such a combination enables one to achieve a multifold increase in sensitivity when compared with a system having just one nonmagnetic metal layer.

Index Terms—**Magneto-optical material, periodic structure, plasmonic nanorods, scattering.**

I. Introduction

INTERACTION of light with the metallic nanostructures and nanoparticles gives rise to various unique effects in photonics and optoelectronics [1]. Research of surface plasmons and their excitation is of interest in the studies of metamaterials, optical antennas, and photonic crystals [2]. The enhanced surface plasmon resonance in noble metallic systems at optical frequencies is expected to be a promising issue for realizing excellent scatterers and absorbers of the visible light [3], [4]. Studies of magneto-optical effects in structures satisfying the conditions of exciting surface plasmons show a promise for a use of sandwiched structures, where the metal layer supporting surface plasmons is in contact with a layer possessing magnetically induced anisotropy [5]–[8]. This research direction has a practical motivation; anisotropic nanostructures are promising for applications in both linear and nonlinear optics. Studies of nanostructures with magnetic properties by optical methods are motivated by the possibilities of their applications in magnetophotonic crystals, where functionalities that cannot be realized with isotropic materials (e.g., nonreciprocical propagation of optical signals, isolators, circulators, optical modulators, and so on) are possible, in recording media, in medicine, and others.

In this regard, scattering of plane wave by grating of the metal (Ag) nanocylinders coupled to the magneto-optical slab is rigorously investigated utilizing the recursive algorithm [9], [10] combined with the Lattice Sums technique [11], [12]. As a magneto-optical slab, we consider Bi-substituted gadolinium iron garnet (Bi:GIG) and measured it experimentally in the laboratory at the VSB-Technical University of Ostrava. The diagonal and off-diagonal components of the dielectric permittivity tensor of the garnet (Bi:GIG) are obtained based on ellipsometric measurements. In the near infrared region, the magneto-optical garnets are commonly used for their sufficiently large magneto-optical effect, low optical absorption, and compatibility with III–V semiconductors and silicon technology. The films of Bi:GIG were grown by liquid phase epitaxy (LPE).

The main advantage of our self-contained formulation is that, first, we extract the reflection and transmission matrices of a single planar array and then obtain the scattering characteristics of the whole structure (grating and the magneto-optical slab) by using a recursive formula. The method is computationally fast, since the recursive relation is based on the simple matrix multiplication. In the formulation, we consider all Floquet modes and their interactions through the scattering by grating and magneto-optical material [9]–[12]. Based on the developed formulation, first, the power reflection coefficient of the structure is numerically studied. Near-field distributions are investigated at the particular wavelengths corresponding to the resonance wavelengths of spectral response in reflectance. A physical insight is given to a coupling between the grating and magneto-optical material. In particular, a strong enhancement of the field inside the magneto-optical material occurs when the scattered harmonic (evanescent harmonic) by the grating is in phase matching with the guided mode supported by the magneto-optical slab.

Finally, it should be noted that our proposed formulation can be easily generalized to study the multilayer structure composed of the magneto-optical and metal films or gratings.

Manuscript received August 13, 2016; revised November 20, 2016; accepted December 27, 2016. Date of publication December 30, 2016; date of current version March 16, 2017. Corresponding author: V. Jandieri (e-mail: vakhtang.jandieri@uni-due.de).

Color versions of one or more of the figures in this paper are available online at http://ieeexplore.ieee.org.

Digital Object Identifier 10.1109/TMAG.2016.2646665

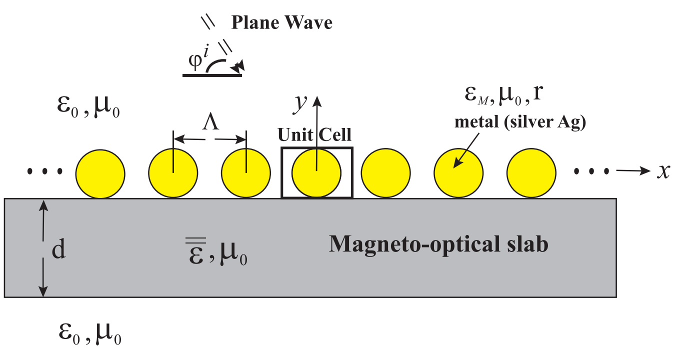

Fig. 1. Cross-sectional view of the grating composed of the metal (Ag) nanocylinders located on the magneto-optical slab having thickness d. Material constants of the metal and the magneto-optical slab are denoted by $(\varepsilon_M, \mu_0, r)$ and $(\bar{\bar{\varepsilon}}, \mu_0)$, respectively. Excitation by a plane wave (H_z, E_x, E_y) with an incident angle φ^i is considered.

The formulation is straightforward. Such kinds of structures are usually used as the magneto-optical surface plasmon resonance sensors. The authors believe that the developed self-contained approach is important for sensing the magneto-optical material by the spectroscopic analysis to define its unknown parameters.

II. Formulation of the Problem

The cross section of the grating with a period Λ composed of the metal nanocylinders per unit cell and located on the magneto-optical slab having thickness d is illustrated in Fig. 1. The structure is situated in a free space. Radius of metal nanocylinders is r and material constants of the metal and magneto-optical slab are denoted by (ε_M, μ_0) and $(\bar{\bar{\varepsilon}}, \mu_0)$, respectively. The structure is illuminated by a plane wave of unit amplitude. The angle of incidence of the plane waves with respect to the$x$-axis is denoted by φ^i. Since we are interested in the scattering problem related to the plasmon resonances that are excited in the case of magnetic field **H** parallel to the z-axis, we focus our investigation on the scattering of plane waves with (H_z, E_x, E_y) components. The time dependence is assumed $\exp(-i\omega t)$ and is omitted in the manuscript.

Magneto-optical slab in the case of transverse magnetization (magnetization is perpendicular to the plane of incidence) is characterized by the tensor dielectric permittivity [13]

$$\bar{\bar{\varepsilon}} = \varepsilon_0 \begin{pmatrix} \varepsilon_\perp & \varepsilon_\times & 0 \\ -\varepsilon_\times & \varepsilon_\perp & 0 \\ 0 & 0 & \varepsilon_\perp \end{pmatrix} \tag{1}$$

where both $\varepsilon_\perp(\lambda)$ and $\varepsilon_\times(\lambda)$ are the complex values and are functions of the wavelength λ (wavelength in a free space). Note that in the numerical analyses in Section III, we use the data for the diagonal $\varepsilon_\perp(\lambda)$ and off-diagonal $\varepsilon_\times(\lambda)$ components of the dielectric permittivity obtained based on our experimental measurements. Substituting (1) into Maxwell's equations, the wave equation for the magnetic field in the magneto-optical slab is derived as follows:

$$\frac{\partial^2 H_z}{\partial x^2} + \frac{\partial^2 H_z}{\partial y^2} + k_0^2 \varepsilon_{MO} H_z = 0 \tag{2}$$

where $k_0 = \omega\ (\varepsilon_0\mu_0)^{1/2}$ and $\varepsilon_{MO} = (\varepsilon_\perp^2 + \varepsilon_\times)^2/\varepsilon_\perp$. In order to rigorously and accurately study the electromagnetic scattering by the plasmonic grating coupled to the magneto-optical medium, we use the Lattice Sums technique combined with the generalized reflection matrix method. The details of the method are omitted in the paper, because it has been already published by the authors in their early works [9]–[12], [14]. The main idea of the formulation could be briefly described as follows: for each planar array (in our case, the structure shown in Fig. 1 is composed of two planar arrays: grating and magneto-optical slab), a multiple scattering process is described in terms of the reflection and transmission matrices that relate the amplitudes of the reflected and transmitted space harmonics to the amplitude of the upgoing and downgoing incident waves. Then, successively concatenating the reflection and transmission matrices for each generalized reflection and transmission matrices are obtained by planar array (grating and the magneto-optical slab) using a recursive formula based on a simple matrix multiplication. In our formulation, we take into account all Floquet modes and their interactions through the scattering by each array. It should be noted that we have very recently successfully applied our method to accurately study the electromagnetic scattering by the plasmonic grating of the metal-coated nanocylinders coupled to the pure dielectric semi-infinite medium [14]. However, the case is quite different for the structure composed of the plasmonic grating and the magneto-optical slab. This is because the off-diagonal elements of the dielectric permittivity of the magneto-optical slab break the up–down symmetry of the reflection and transmission matrices and lead to the appearance of additional terms in the expressions for the reflection and transmission matrices characterizing the upgoing and downgoing space harmonics from/on the magneto-optical slab. The space-harmonics scattered by the grating propagate in upward and downward directions inside the magneto-optical slab and are scattered at the plane boundaries between the slab and the free space. The schematic of this process is demonstrated in Fig. 2. In the case of magneto-optical slab with tensor dielectric permittivity, the Fresnel reflection and transmission matrices are expressed in the following form:

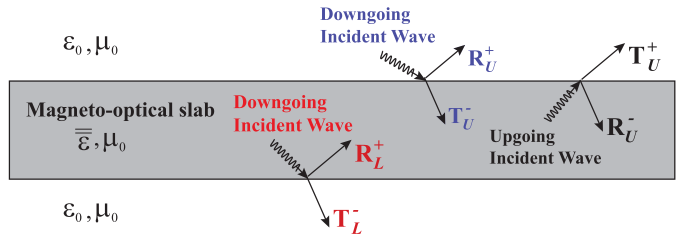

Fig. 2. Schematic of the reflection and transmission of the space harmonics at the plane boundaries between the magneto-optical slab and the free space.

$$\mathbf{T}_L^- = [T_{L,\ell}^- \delta_{\ell\ell'}] = \left[\frac{2\tilde{k}_{y\ell}}{\tilde{k}_{y\ell} + \varepsilon_{MO} k_{y\ell} + k_{x\ell}\varepsilon_\times/\varepsilon_\perp} \right] \tag{3}$$

$$\mathbf{R}_U^+ = [R_{U,\ell}^+ \delta_{\ell\ell'}] = \left[\frac{\varepsilon_{MO} k_{y\ell} - \tilde{k}_{y\ell} + k_{x\ell}\varepsilon_\times/\varepsilon_\perp}{\varepsilon_{MO} k_{y\ell} + \tilde{k}_{y\ell} - k_{x\ell}\varepsilon_\times/\varepsilon_\perp} \right] \tag{4}$$

$$\mathbf{T}_U^- = [T_{U,\ell}^- \delta_{\ell\ell'}] = \left[\frac{2\varepsilon_{MO} k_{y\ell}}{\varepsilon_{MO} k_{y\ell} + \tilde{k}_{y\ell} - k_{x\ell}\varepsilon_\times/\varepsilon_\perp} \right] \tag{5}$$

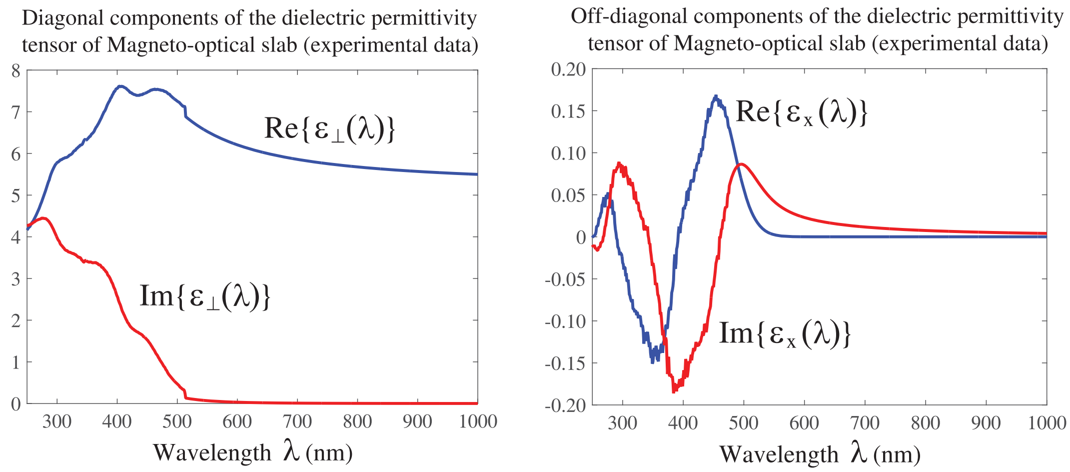

Fig. 3. Diagonal and off-diagonal components of the dielectric permittivity tensor of the Bi-substituted gadolinium iron–garnet (Bi:GIG) obtained by ellipsometric measurements in the wavelength range 250 nm $< \lambda <$ 1000 nm.

$$\mathbf{R}_U^- = [R_{U,\ell}^- \delta_{\ell\ell'}] = \left[\frac{\tilde{k}_{y\ell} - \varepsilon_{MO} k_{y\ell} + k_{x\ell}\varepsilon_\times/\varepsilon_\perp}{\tilde{k}_{y\ell} + \varepsilon_{MO} k_{y\ell} - k_{x\ell}\varepsilon_\times/\varepsilon_\perp}\right] \quad (6)$$

$$\mathbf{T}_U^+ = [T_{U,\ell}^+ \delta_{\ell\ell'}] = \left[\frac{2\tilde{k}_{y\ell}}{\tilde{k}_{y\ell} + \varepsilon_{MO} k_{y\ell} - k_{x\ell}\varepsilon_\times/\varepsilon_\perp}\right] \quad (7)$$

where

$$k_{x\ell} = k_0 \cos\varphi_\ell = k_0\left(\cos\varphi^i + \frac{2\pi\ell}{k_0\Lambda}\right) \quad (8)$$

$$k_{y\ell} = k_0 \sin\varphi_\ell = k_0\sqrt{1-\cos^2\varphi_\ell}, \quad Im\left(k_{y\ell}\right) \geq 0 \quad (9)$$

$$\tilde{k}_{y\ell} = k_0\sqrt{\varepsilon_{MO} - \cos^2\varphi_\ell}, \quad Im(\tilde{k}_{y\ell}) \geq 0. \quad (10)$$

Note that when $\varepsilon_\times = 0$, $\mathbf{T}_L^- = \mathbf{T}_U^+$ and $\mathbf{R}_L^+ = \mathbf{R}_U^-$. Since the Fresnel reflection and transmission matrices characterizing the magneto-optical slab are defined, we can implement these matrices into the formulation developed in [14]. Finally, electric and magnetic fields in each region of the structure shown in Fig. 1 can be calculated following the same calculation procedure as in [14]. Thus, the problem is rigorously solved.

III. Numerical Results and Discussions

In the numerical examples in what follow, we assume silver (Ag) for the metal employing the Drude–Lorentz model. Silver is commonly used for nanoparticle plasmonics because of the relatively easy production and relatively small loss. Although the substantial number of the numerical results could be generated, we study an oblique incidence of the plane waves $\varphi^i = 45°$ under the following structural parameters: $r = 40$ nm, $d = 700$ nm, and $\Lambda = 200$ nm. In the numerical results that follows, the truncation number for all vectors and matrices is taken $N = 20$ in order to have a convergence of the numerical solutions. As a magneto-optical slab, we consider Bi:GIG experimentally specified in the laboratory at the VSB-Technical University of Ostrava [15].

The diagonal and off-diagonal components of the dielectric permittivity tensor of the garnet (Bi:GIG) obtained by the ellipsometric measurements are given in Fig. 3 in the wavelength range 250 nm $< \lambda <$ 1000 nm. In the near infrared region, the magneto-optical garnets are commonly used for their sufficiently large magneto-optical effect, low optical

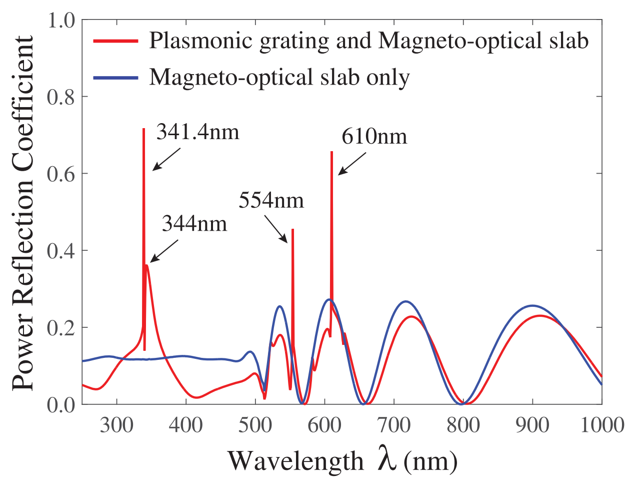

Fig. 4. Power reflection coefficient of the structure composed of the plasmonic grating and magneto-optical slab (red line) and the magneto-optical slab only (blue line) at $\varphi^i = 45°$, $r = 40$ nm, $d = 700$ nm, and $\Lambda = 200$ nm.

absorption, and compatibility with III–V semiconductors and silicon technology. The films of Bi:GIG were grown by LPE. magneto-optical garnet films have applications as optical waveguides with signal modulation too. By LPE, the bubble garnets films (with thicknesses less and more 1 μm—single mode and multimode waveguiding, respectively) have been prepared and we published refractive index spectra of these materials resulting from the combination of guided modes technique at 1152.3 and 632.8 nm wavelengths and reflection interference spectroscopy [16].

When pure metal (Ag) nanocylinders are periodically distributed along the x-axis, the grating is formed. The normalized power reflection coefficient is demonstrated in Fig. 4 by the red line. For comparison, the reflection coefficient only of the magneto-optical slab is shown by the blue line. First, let us focus on the resonances that appear in the spectral response (red line). Since we are dealing with the incidence of the plane waves on the periodic structure, we can observe the Rayleigh anomaly ($k_{y\ell} = 0 \Rightarrow \ell(\lambda/\Lambda) = -\cos\varphi^i \pm 1$) related to the periodic nature of the grating at 341.4 nm ($\ell = -1$). A resonance peak in the shorter wavelength region

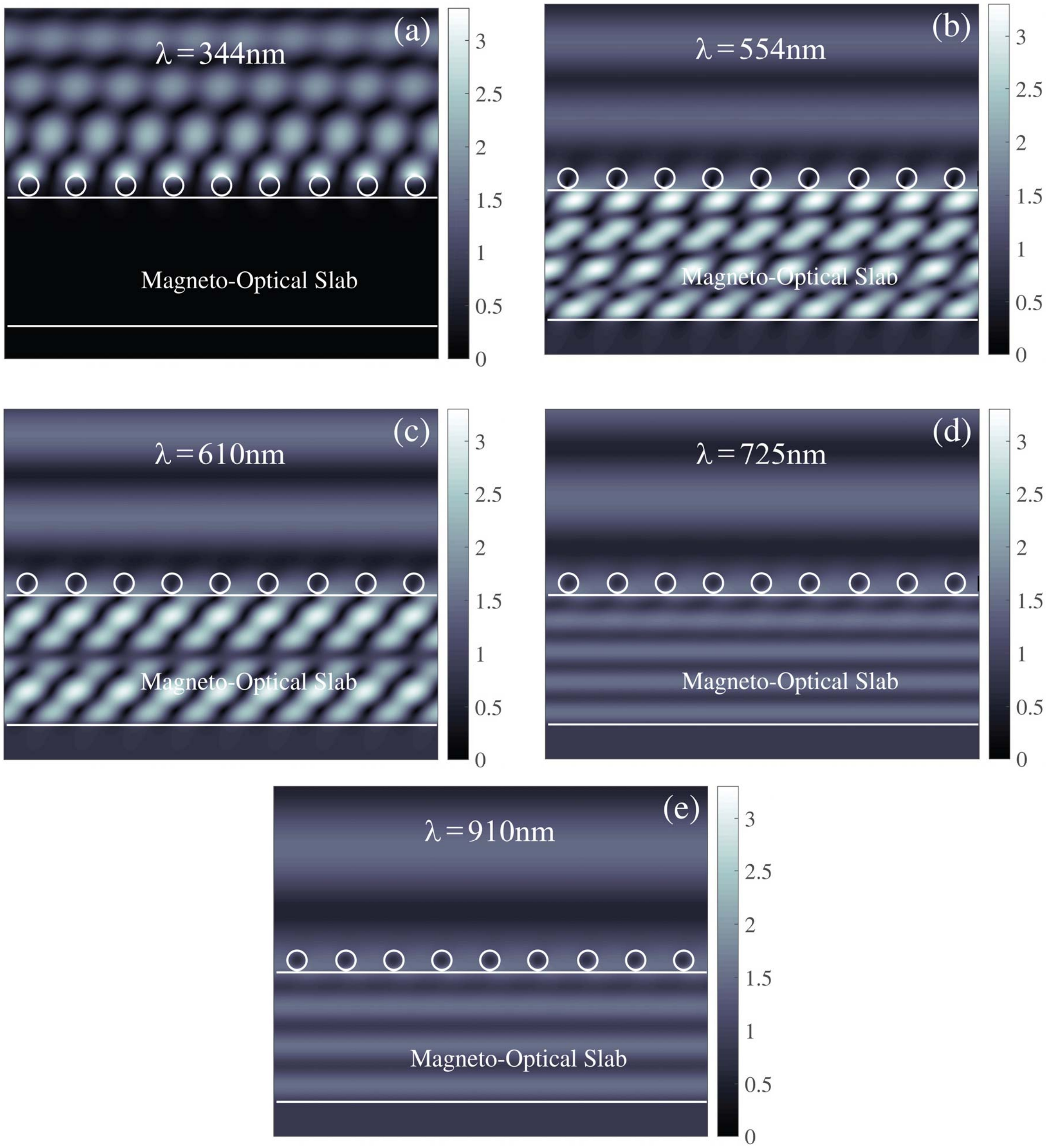

Fig. 5. Near-field distribution $|H_z|$ at some particular wavelengths of spectral response (Fig. 4).

that appears at 344 nm is related to the resonance of a single plasmon nanorod and it is independent of the characteristics of the magneto-optical slab (note that no resonance peaks are observed in the short wavelength region when only magneto-optical slab is considered).

In addition, there are two pronounced resonance peaks at 554 and 610 nm, whereas no resonance peaks are observed in the absence of the grating (blue line). These resonance dips represent the guided mode resonances, which occur when the scattered wave of the ℓth diffraction order is in phase matching with the guided modes supported by the magneto-optical slab. In other words, the physics of the resonance peaks at 554 and 610 nm is as follows: the incident plane wave is scattered into a set of space harmonics some of which become to be evanescent in the y-direction. When the phase matching condition between the guided optical wave (guided mode) and one of the evanescent space harmonic is fulfilled at some wavelength, these two evanescent wave components effectively interact and a fraction of power of the incident wave is resonantly transferred to the power of guided wave along the slab waveguide. Such a resonant interaction produces a sharp dip in the spectral response of power reflection coefficient at some particular wavelength. The phase matching conditions for the resonant interaction are given as follows:

$$\frac{d}{\lambda} = \frac{1}{\pi\sqrt{\varepsilon_{MO} - \left(\frac{\beta\lambda}{2\pi}\right)^2}} \times \left[\tan^{-1}\left(\varepsilon_{MO}\sqrt{\frac{\left(\frac{\beta\lambda}{2\pi}\right)^2 - 1}{\varepsilon_{MO} - \left(\frac{\beta\lambda}{2\pi}\right)^2}}\right) + m\frac{\pi}{2}\right] \quad (m = 0, 1, 2, \cdots) \tag{11}$$

$$\beta \approx k_0 \cos\varphi^i + \frac{2\pi}{\Lambda}\ell \ (\ell = \pm 1, \pm 2, \pm 3, \cdots) \tag{12}$$

where β is the propagation constant of the guided wave in the slab. Calculating β based on (12) and substituting it into (11), we have seen that the phase matching condition is fulfilled at 554 nm when $\ell = -1$ and $m = 3$ and at 610 nm when $\ell = -1$ and $m = 1$.

Finally, we can observe two maxima in the longer wavelength region at 725 and 910 nm. They are defined exclusively by the existence of magneto-optical slab. From the Fig. 4, it follows that the maxima are slightly shifted to the longer wavelength region by the existence of the plasmonic grating; however, it should be noted that no coupling occurs between the grating and the magneto-optical slab at these wavelengths.

It is obvious that by changing the geometrical parameters of the structure, the spectral response (resonance wavelengths) will be changed. In this regard, we have conducted several numerical tests by varying the geometrical parameters of the grating (a radius of the nanorods and a period of the grating) and the magneto-optical medium (a thickness of the slab), as well as the angle of wave incidence. However, no new resonance phenomena have been observed.

In order to give a physical insight into the analyses of the spectral responses, we calculate the near field distributions $|H_z|$ at some particular wavelengths shown in Fig. 4. The circles depicted by white lines indicate the boundary surface of the metal (Ag) nanocylinders and the white lines indicate the boundaries of the magneto-optical slab. Fig. 5(a) demonstrates the near-field distribution at the resonance wavelength 344 nm. From this figure, it follows that the resonance wavelength 344 nm corresponds to the resonance of the single plasmon nanorod. A strong field is excited in the illuminated side on the boundaries of the plasmon nanocylinders and the multiple interaction between the nanorods is barely seen. On the other hand, the field inside the magneto-optical slab is almost zero, which is caused by the strong damping effect of the waves (note that the imaginary part of the dielectric permittivity is quite large in the short wavelength region as it is shown in Fig. 3). Fig. 5(b) and (c) shows the near-field distributions at the wavelengths 554 and 610 nm, respectively, when the scattered waves are resonantly coupled to the guided modes in the magneto-optical slab. From the figures, it follows that the field is strongly enhanced inside the magneto-optical slab due to the interaction between the plasmon nanorods and the magneto-optical material. For comparison, the near-field distributions at 725 and 910 nm, when no coupling occurs between the grating and the slab, are also illustrated in Fig. 5(d) and (e).

Finally, it should be noted that our proposed formulation can be easily generalized to study the multilayer structure composed of the magneto-optical and metal films or gratings. The formulation is straightforward. Such kinds of structures are usually used as magneto-optical surface plasmon resonance sensors. Studies of magneto-optical effects in structures satisfying the conditions of exciting surface plasmons (MO SPR structures) show a promise for a use of sandwiched structures (multilayers, gratings) where the metal layer supporting SPPs is in contact with a layer possessing magnetically induced anisotropy. Such a combination enables one to achieve a multifold increase in response when compared with a system having just one nonmagnetic metal layer.

IV. Conclusion

The rigorous and accurate formulation for the wave scattering by a plasmonic grating of the nanorods coupled to the magneto-optical slab is presented. Bi:GIG is considered as the magneto-optical material. Its material properties are measured experimentally and used in our analyses. Near-field distributions at the particular resonance wavelengths in the spectral response in reflectance related to the surface plasmon and the coupling between the plasmonic grating and the magneto-optical slab have been numerically studied. Special attention has been paid to the field enhancement in the magneto-optical material due to the interaction with the plasmonic grating. The formulation proposed in this paper can be applied to various configurations with different magnetic materials and different types of excitation sources.

The authors believe that the developed self-contained approach could be also important for sensing the magneto-optical medium. In particular, when the parameters of the magneto-optical material are unknown, those may be sensed or measured by using the spectroscopic analysis of the scattered field through a grating structure coupled to the magneto-optical sample. If the spectral responses are accurately formulated by using a self-contained approach, we can sense and predict the material parameters of the magneto-optical material from the measured data on the scattered field.

Acknowledgment

This work was supported in part by the Shota Rustaveli National Science Foundation under Grant 216662 and Grant FR/25/6-100/14 and in part by the Grand Agency of the Czech Republic under Grant #15-21547S. The work of V. Jandieri was supported by the Alexander von Humboldt Foundation.

References

[1] P. Berini, "Long-range surface plasmon polaritons," *Adv. Opt. Photon.*, vol. 1, no. 3, pp. 484–588, 2009.

[2] O. Hess, J. B. Pendry, S. A. Maier, R. F. Oulton, J. M. Hamm, and K. L. Tsakmakidis, "Active nanoplasmonic metamaterials," *Nature Mater.*, vol. 11, pp. 573–584, Jun. 2012.

[3] V. G. Kravets, F. Schedin, and A. N. Grigorenko, "Extremely narrow plasmon resonances based on diffraction coupling of localized plasmons in arrays of metallic nanoparticles," *Phys. Rev. Lett.*, vol. 101, p. 087403, Aug. 2008.

[4] B. S. Luk'yanchuk and V. Ternovsky, "Light scattering by a thin wire with a surface-plasmon resonance: Bifurcations of the Poynting vector field," *Phys. Rev. B, Condens. Matter*, vol. 73, p. 235432, Jun. 2006.

[5] B. J. H. Stadler and T. Mizumoto, "Integrated magneto-optical materials and isolators: A review," *IEEE Photon. J.*, vol. 6, no. 1, Feb. 2013, Art. no. 0600215.

[6] V. I. Belotelov *et al.*, "Enhanced magneto-optical effects in magnetoplasmonic crystals," *Nature Nanotechnol.*, vol. 6, pp. 370–376, Apr. 2011.

[7] V. A. Kosobukin, "Near-field magnetooptics in resonant light scattering by a linear nanoprobe," *Tech. Phys. Lett.*, vol. 34, no. 10, pp. 857–860, 2008.

[8] N. A. Gusev, V. I. Belotelov, and A. K. Zvezdin, "Surface plasmons in nanowires with toroidal magnetic structure," *Opt. Lett.*, vol. 39, no. 14, pp. 4108–4111, 2014.

[9] V. Jandieri, K. Yasumoto, and Y. Liu, “Directivity of radiation of a dipole source coupled to cylindrical electromagnetic bandgap structures,” *J. Opt. Soc. Amer. B, Opt. Phys.*, vol. 29, no. 9, pp. 2622–2629, 2012.

[10] V. Jandieri and K. Yasumoto, “Electromagnetic scattering by layered cylindrical arrays of circular rods,” *IEEE Trans. Antennas Propag.*, vol. 59, no. 6, pp. 2437–2441, Jun. 2011.

[11] K. Yasumoto, H. Toyama, and T. Kushta, “Accurate analysis of two-dimensional electromagnetic scattering from multilayered periodic arrays of circular cylinders using lattice sums technique,” *IEEE Trans. Antennas Propag.*, vol. 52, no. 10, pp. 2603–2611, Oct. 2004.

[12] K. Yasumoto, Ed., *Electromagnetic Theory and Applications for Photonic Crystals*. Boca Raton, FL, USA: CRC Press, 2005.

[13] K. Postava, J. Pištora, Š. Višňovský, “Magneto-optical effects in ultrathin structures at transversal magnetization,” *Czechoslovak J. Phys.*, vol. 49, no. 8, pp. 1185–1204, 1999.

[14] V. Jandieri, P. Meng, K. Yasumoto, and Y. Liu, “Scattering of light by gratings of metal-coated circular nanocylinders on a dielectric substrate,” *J. Opt. Soc. Amer. A, Opt. Image Sci.*, vol. 32, no. 7, pp. 1384–1389, 2015.

[15] L. Halagačka *et al.*, “Mueller matrix optical and magneto-optical characterization of Bi-substituted gadolinium iron garnet for application in magnetoplasmonic structures,” *Opt. Mater. Exp.*, vol. 4, no. 9, pp. 1903–1919, 2014.

[16] J. Pištora, Š. Višňovský, K. Nitsch, V. Pařízek, V. Prosser, “Refractive index of 2-μm bubble garnet films,” *J. Appl. Phys.*, vol. 53, no. 12, pp. 9002–9004, 1982.